HHS Public Access

Author manuscript

J Leukoc Biol. Author manuscript; available in PMC 2019 May 01.

Published in final edited form as:

J Leukoc Biol. 2018 May ; 103(5): 919–932. doi:10.1002/JLB.3A0617-252RR.

Phospholipase D isoforms differentially regulate leukocyte responses to acute lung injury

Raja-Elie E. Abdulnour[1], **Judie A. Howrylak**[2], **Alexander H. Tavares**[1], **David N. Douda**[1], **Karen M. Henkels**[3], **Taylor E. Miller**[3], **Laura E. Fredenburgh**[1], **Rebecca M. Baron**[1], **Julian Gomez-Cambronero**[3,4], and **Bruce D. Levy**[1,4]

[1]Division of Pulmonary and Critical Care Medicine, Brigham and Women's Hospital, Harvard Medical School, Boston, Massachusetts, USA

[2]Division of Pulmonary Allergy and Critical Care Medicine, Penn State Hershey Medical Center, Hershey, Pennsylvania, USA

[3]Department of Biochemistry and Molecular Biology, Wright State University, Dayton, Ohio, USA

[4]Center for Experimental Therapeutics and Reperfusion Injury, Brigham and Women's Hospital, Harvard Medical School, Boston, Massachusetts, USA

Abstract

Phospholipase D (PLD) plays important roles in cellular responses to tissue injury that are critical to acute inflammatory diseases, such as the acute respiratory distress syndrome (ARDS). We investigated the expression of PLD isoforms and related phospholipid phosphatases in patients with ARDS, and their roles in a murine model of self-limited acute lung injury (ALI). Gene expression microarray analysis on whole blood obtained from patients that met clinical criteria for ARDS and clinically matched controls (non-ARDS) demonstrated that PLD1 gene expression was increased in patients with ARDS relative to non-ARDS and correlated with survival. In contrast, PLD2 expression was associated with mortality. In a murine model of self-resolving ALI, lung *Pld1* expression increased and *Pld2* expression decreased 24 h after intrabronchial acid. Total lung PLD activity was increased 24 h after injury. *Pld1*$^{-/-}$ mice demonstrated impaired alveolar barrier function and increased tissue injury relative to WT and *Pld2*$^{-/-}$, whereas *Pld2*$^{-/-}$ mice demonstrated increased recruitment of neutrophils and macrophages, and decreased tissue injury. Isoform-specific PLD inhibitors mirrored the results with isoform-specific *Pld*-KO mice. PLD1

Correspondence: Bruce D. Levy, Brigham and Women's Hospital, Division of Pulmonary and Critical Care Medicine, 60 Fenwood Rd, Boston, MA 02115, USA. blevy@partners.org.

AUTHORSHIP

R.E.A. contributed to experimental design, carried out experiments and data analyses, and wrote the manuscript; J.A.H. contributed to experimental design, carried out experiments and data analysis, and contributed to manuscript and figure preparation; A.H.T., D.N.D., K.M.H., and T.E.M. carried out experiments and data analysis and contributed to manuscript and figure preparation; L.E.F., R.M.B., and J.G.C contributed to experimental design, data analysis, and manuscript preparation; B.D.L. contributed to experimental design, carried out experiments and data analyses, contributed to manuscript preparation, and conceived the overall research plan.

All authors concur with the submission and none of the data has been previously reported or is under consideration for publication elsewhere

SUPPORTING INFORMATION

Additional Supporting Information may be found online in the supporting information tab for this article.

DISCLOSURES

The authors declare no conflicts of interest.

gene expression knockdown in human leukocytes was associated with decreased phagocytosis by neutrophils, whereas reactive oxygen species production and phagocytosis decreased in M2-macrophages. PLD2 gene expression knockdown increased neutrophil and M2-macrophage transmigration, and increased M2-macrophage phagocytosis. These results uncovered selective regulation of PLD isoforms after ALI, and opposing effects of selective isoform knockdown on host responses and tissue injury. These findings support therapeutic strategies targeting specific PLD isoforms for the treatment of ARDS.

Keywords

acute lung injury; acute respiratory distress syndrome; microarray; Phospholipase D

1 | INTRODUCTION

Dysregulated inflammation and altered permeability of alveolar endothelial and epithelial barriers remain central to the pathophysiology of the acute respiratory distress syndrome (ARDS). Despite significant progress in our understanding of ARDS pathogenesis, therapeutic modalities are limited and mortality remains unacceptably high.[1]

Neutrophils are the first responders to sites of tissue injury to contain and eliminate invading pathogens via intra- and extracellular mechanisms, such as phagocytosis and release of proteases, oxidants, antimicrobial peptides, and neutrophil-extracellular traps (NETs).[2] Resident and recruited macrophages participate in these initial inflammatory responses, and orchestrate resolution of inflammation by clearing dead cells and initiating tissue repair.[3] In health, regulation of these inflammatory responses ensures a prompt return to homeostasis. As such, excessive neutrophil activation and impaired clearance of the inflammatory milieu can potentiate tissue injury and cause human disease, such as ARDS.[4]

Phospholipase D (PLD) is necessary for cellular responses to tissue injury and microbial invasion,[5] including leukocyte adhesion,[6] and phagocytosis.[7] Cellular models have shown that PLD1 is highly expressed in leukocytes and regulates several aspects of acute inflammatory responses, including oxidative burst.[8] PLD2 plays important roles in regulating phagocytosis and cell replication.[9] Both PLD1 and PLD2 are necessary for leukocyte chemotaxis.[10] An experimental model of acute pancreatic injury has shown that PLD1 and PLD2 regulate leukocyte recruitment to inflamed tissue and edema formation.[11] In a sepsis model with secondary lung injury, PLD2 deficiency afforded lung protection and increased survival.[12] Here, we examined PLD involvement in host responses to the important clinical problem of ARDS.

The enzymatically active isoforms of the PLD superfamily, PLD1 and PLD2, hydrolyze phosphatidylcholine to generate choline and phosphatidic acid (PA). The PA generated via PLD activity can play multiple roles in cellular function.[13] PA can function in signal transduction events, such as activation of a phosphoinositide kinase, or as a lipid-binding partner to several proteins. In addition, PA production is important in vesicle trafficking, endocytosis, and secretion. PA can also be further converted by PA phosphatases to diacylglycerol, which also signals for cellular processes important to inflammation and

tissue repair.[14] Apart from its metabolic functions, PLD can also regulate select cellular functions through direct interactions with other proteins.[7]

Results presented here show that PLD1 expression increased in ARDS patients and was associated with survival. In a murine model of self-resolving ALI, PLD1 gene expression in injured lungs increased, whereas PLD1 deficiency worsened ALI severity by alveolar barrier disruption and decreased macrophage phagocytosis. In contrast, PLD2 expression was associated with mortality in ARDS patients, and PLD2 expression decreased in murine self-resolving ALI. PLD2 deficiency lessened ALI severity, and was associated with increased recruitment of macrophages with enhanced phagocytosis and decreased neutrophil production of reactive oxygen species (ROS). Together, these findings have uncovered counter-regulation by PLD isoforms that influence the nature and severity of tissue injury.

2 | MATERIALS AND METHODS

2.1 | Registry of Critical Illness

Details of the Research Registry and Human Sample Repository for the Study of the Biology of Critical Illness, abbreviated as the Registry of Critical Illness (RoCI), have been previously published.[15] The RoCI collects demographic, clinical information, and blood specimens from patients with critical illness in the medical intensive care unit of the Brigham and Women‘s Hospital (BWH). RoCI is approved by the Partners Human Research Committee and operates under protocol 2008-P-000495.

Patients are classified by the treating intensive care physician team as sepsis, and sepsis with ARDS (sepsis/ARDS). Sepsis was identified according to the 2001 SCCM/ESICM/ACCP/ATS/SIS International Sepsis Definitions Conference guidelines.[16] ARDS was defined according to American-European Consensus Conference on ARDS guidelines.[17] All ARDS patients were endotracheally intubated and mechanically ventilated using a low tidal volume ventilation strategy according to ARDSNet protocol.[18] The following parameters were collected for each patient for further analyses: age, race, gender, length of hospital stay, APACHE II score, in-hospital mortality, 28-day mortality and overall mortality. APACHE II was calculated on intensive care unit (ICU) admission day for every patient,[19] and mortality was assessed using the Partners Health Care Research Patient Data Registry (RPDR) linking deaths to the Social Security Death Index (SSDI).

2.2 | Human microarray datasets

Peripheral blood with corresponding demographic and clinical information was obtained from adult patients were obtained from subjects enrolled in the RoCI at the Brigham and Women’s Hospital ICU.[15] Samples were also obtained from adult patients in the University of Pittsburgh Medical Center ICU,[20] and pediatric patients (< 10 years old) admitted to the Cincinnati Children’s Hospital pediatric ICU.[21]

2.3 | Microarray preprocessing, normalization, and analysis

All preprocessing and analysis of linear correlation between gene expression levels, ARDS diagnosis, and 28-day survival after adjustment for age, sex, race, and age were performed in

R 3.2/Bioconductor.[22,23] To evaluate the concordance of gene expression patterns across different microarray platforms, we mapped each microarray probe to its genomic coordinates on the UCSC Human Genome version 18 (hg18) using the R/Bioconductor *biomaRt* package.[24,25] We next matched probes to those on different platforms using the nearest genomic start position and filtering out probes that were not represented across all platforms.[25,26] The number of probes in the pooled dataset carried forward for normalization was 18,694. We used the R package, *CONOR*, to perform distance weighted discrimination cross-platform normalization, to account for differences in probe length, probe type, number of probes, labeling methods, and detection methods.[27] PLD genes are expressed as PLD1 and PLD2 in humans, and *Pld1, Pld2* in murine datasets.

2.4 | Mice

C57BL/6 (18–22 week old, male:female ratio 1:1, body weights 20–25 g; Charles River Laboratories, Wilmington, MA), *Pld1*$^{-/-}$ and *Pld2*$^{-/-}$ were housed in isolation cages in pathogen-free conditions on a light-dark cycle with light from 7:00 to 20:00 at 25°C. *Pld1*$^{-/-}$ and *Pld2*$^{-/-}$ were obtained from Dr. Gilbert Di Paolo (Department of Medicine, College of Physicians and Surgeons, Columbia University, New York, New York)[28] and Dr. Yasunori Kanaho (Department of Physiological Chemistry, University of Tsukuba, Tsukuba, Japan).[29] The *Pld1*$^{-/-}$ and *Pld2*$^{-/-}$ mice were backcrossed with C57bl/6 mice for > 7 generations.[29,30] Mice were fed a standard diet (Laboratory Rodent Diet 5001; PMI Nutrition International, St. Louis, MO) containing 4.5% total fat with 0.3% ω-3 fatty acids and <0.02% C20:4 and were provided water ad libitum.

2.5 | Murine model of acid-induced acute lung injury

All mice were maintained under specific pathogen-free conditions. All studies were reviewed and approved by the Harvard Medical Area standing committee on animals (protocol no. 03618). Mice were anesthetized with i.p. injections of ketamine (100 mg/kg body wt; Phoenix Scientific, St. Joseph, MO) and xylazine (10 mg/kg body wt; Phoenix Scientific). As in Abdulnour et al.,[31] hydrochloric acid (0.1 N HCl, pH 1.5, 50 μ*L*, endotoxin free; Sigma–Aldrich, St Louis, MO) was instilled selectively into the left mainstem bronchus via a 24-G angio-catheter inserted intratracheally.

2.6 | Preparation of lung samples prior to quantitative real-time PCR, Western blot, and PLD activity determinations

Left lungs from C57BL/6 mice of 3 genotypes (WT, PLD1$^{-/-}$, or PLD2$^{-/-}$) were injured with 0.1 N HCl intrabronchially. Lungs were collected at time zero (no injury) and at 24 h after injury, cut longitudinally and flash frozen. On the day of the analyses, tissue samples were weighed and an appropriate volume (between 70 and 120 μL) of lysis buffer (for Western blot or PLD enzyme assays) or buffer A from RNeasy mini kit (for quantitative real-time PCR[qRT-PCR] assays) was added to reach ~1 mg/mL solutions. Lysis buffer composition for Western blots and enzyme assays was: 50 mM HEPES, pH 7.2,100 μM Na_3VO_4, 0.1% Triton X-100 and 1 mg/mL each of protease inhibitors (aprotonin and leupeptin). Lung tissue was ground with a micromotorized pestle homogenizer, followed by sonication (10 s) on ice. Samples were spun for 5 min at 250 × *g* on a refrigerated centrifuge (4°C) to remove debris and supernatants were taken for further analyses

2.7 | Gene expression measurement by qRT-PCR

Reverse transcription coupled to qPCR was performed following published technical details.[32] Total RNA was isolated from cells with the RNeasy minikit per the manufacturer's protocol (Qiagen, Valencia, CA). RNA concentrations were determined using a NanoDrop 2000c UV-Vis Spectrophotometer (Thermo Scientific, Wilmington, DE) and samples were normalized to a fixed concentration of 50 ng/μL RNA. Reverse transcription was performed with 210 ng RNA, 210 ng random hexamers, 500 μM dNTPs, 84 U RNase OUT and 210 units of Superscriptll reverse transcriptase (Life Technologies, Carlsbad, CA) and incubated at 42°C for 55 min. All qPCR reactions were run with 100 ng total input RNA, 2 μL of PLD1 gene expression assay (FAM-labeled) or 2 μL of the PLD2 gene expression assay (FAM-labeled) multiplexed with the housekeeping gene (β-Actin) (FAM-labeled) with the final concentrations being 200 pmol and 400 pmol for the primers and probe, respectively. All primers and fluorescent probes were synthesized by ThermoFisher Scientific (Life Technologies). The qPCR conditions for the Stratagene Cycler were: 95°C for 3 min and then 50 cycles of the next 3 steps: 30 s 95°C, 1 min 60°C, and then 1 min 72°C. The "cycle threshold" Ct values were chosen from the linear part of the PCR amplification curves where an increase in fluorescence is detected at >10 S.E.M. above the background signal, and referred to housekeeping gene (GAPDH).

2.8 | Phospholipase activity assay

The measurement of total PLD activity was reported previously.[6,33] Briefly, the assay was performed in liposomes of 1,2-dioctanoyl-sn-glycero-3-phosphocholine (PC8) and [3H]-butanol. The following reagents (final concentrations): 3.5 mm PC8 phospholipid, 45 mM HEPES, pH 7.8, and 1.0 μCi of n-[3H]-butanol were added in a liposome form as indicated in.[34] Samples were incubated for 20 min at 30°C with continuous shaking. The addition of 0.3 mL of ice-cold chloroform/methanol (1:2) stopped the reactions. Lipids were isolated, dried (under N2) and suspended in chloroform:methanol (9:1) and then spotted on thin-layer chromatography plates along with 1,2-dipalmitoyl-sn-glycero-3-phosphobutanol (PBut) (Avanti polar lipids, Inc., AL) authentic standards. The amount of [3H]-phosphatidylbutanol ([3H]-PBut) that co-migrated with PBut standards (Rf~0.45 + 0.36) was measured by scintillation spectrometry and background subtracted. Results were expressed as total PLD enzymatic activity as dpm/mg protein/min.

2.9 | Bronchoalveolar lavage

At timed intervals, mice were euthanized and the trachea exposed. A 20-gauge angiocatheter was inserted into the trachea and the lungs were lavaged with 2 separate 1 mL volumes of ice-cold PBS with 0.6 mM EDTA. The bronchoalveolar lavage (BAL) fluid was pooled, centrifuged at 500 × g for 5 min at 4°C to pellet the cell fraction. The cell pellet was suspended in cold PBS, and the supernatant was used for albumin, protein, and cytokine analysis. BAL neutrophil count was highest at 24 h after ALI (Supplemental Fig. S1 and,[31] therefore that time point was used for determinations after ALI.

2.10 | Assessment of vascular leakage after pharmacologic isoform-specific PLD inhibition

Evans blue dye (EBD, 40 mL/kg) was injected into the tail vein of mice 30 min before termination of the experiment to assess vascular leak. In brief, lungs were lavaged and perfused free of blood with DPBS before being excised *en bloc*. The left lungs were dried in an oven (56°C) for 48 h and weighed. The lungs were then homogenized in DPBS (500 μL), incubated with 2 vol formamide (18 h, 56°C), and centrifuged at 5000 × *g* for 30 min, and the optical density of the supernatant was determined by spectrophotometry at 620 nm. Extravasated EBD in lung homogenates (μg EBD per lung) was calculated with an EBD standard curve. To inhibit PLD isoforms, animals were treated with a specific PLD1 inhibitor (VU0155069),[35] PLD2 inhibitor (VU0364739),[29] or vehicle (saline in 10% vol/vol DMSO) given by intraperitoneal injections on days –3, –2, –1, and 0 (1 h prior to ALI, 10 mg/kg in 10% DMSO).

2.11 | FACS analysis and cell sorting

BAL cells were obtained after centrifugation of pooled BAL fluid, and the cell pellet was stained with fluorochrome-labelled antibodies to obtain a leukocyte differential as in Abdulnour et al.[36]; neutrophils ($CD45^+$ $F4/80^-$ $Ly6G^+$ $CD11b^+$), infiltrating macrophages (iMacs; $CD45^+$ SSc^{High} $F4/80^+$ $CD11c^{Low}$ $CD11b^+$ SiglecF–Ly6C+), exudative macrophages (ExMacs; $CD45^+$ SSc^{High} $F4/80^+$ $CD11c^{High}$ $CD11b^+$ SiglecF+ Ly6C+), and resident alveolar macrophages (rAM; $CD45^+$ $F4/80^+$ SSc^{High} $CD11c^{High}$ $CD11b^-$ SiglecF+ Ly6C−). Cell counts were obtained by adding a known amount of fluorescent counting beads (CountBright; Life Technologies) to the BAL cell pellet prior to flow cytometry as per the manufacturer's recommendations, and normalized to lavage. FACSCanto II (BD Biosciences, San Jose, CA, USA) and FlowJo Ver. 10 software (Tree Star, Ashland, OR) were used for analyses. In some experiments, whole murine lungs were homogenized 24 h after ALI and a cell suspension was prepared as in.[31] Neutrophils (CD45+ Ly6G+), macrophages (CD45+ SSc^{High} F4/80+), lung epithelial cells (CD45− CD31− CD326+), and lung endothelial cells (CD45− CD31+) were sorted with >95% purity, using FACSAria (BD Biosciences, San Jose, CA, USA). The sorted populations were used for RNA extraction and RT-PCR.

2.12 | Determination of bioactive molecule levels in BALF

Select cytokines were measured in aliquots of pooled BALF using a bead-based immunoassay as per the manufacturer's instructions (LEG-ENDPlex by Biolegend, San Diego, CA).

2.13 | Histopathology

Lung tissue was fixed by inflation with Zinc Fixative (BD Pharmingen, San Diego, CA) at a trans-pulmonary pressure of 20 cm H_2O and embedded in paraffin. For histologic analysis, lungs were collected 0, 24, and 48 h after *Escherichia coli* instillation and paraffin-embedded 5-μm sections of lungs were cut and stained with H&E for light microscopy. Leica DFC480 and Leica QWin Standard V3.4.0 (Leica Microsystems Ltd., Buffalo Grove, IL, USA) were used for microscopic analysis.

2.14 | Gene silencing

Human promyelomonocytic HL60 cells were differentiated into neutrophils (CD66b, +CD11b/CD16b+), with 4 days of 1.25% DMSO continuously in culture. Human promonocytic U937 cells were differentiated into macrophages (CD14+,CD68+, CD71+) with 48 h of Vitamin D3 (40 ng/mL) followed by 24 h in control medium (resting period to allow full adhesion). The resulting macrophages were further incubated with 20 ng/mL IL-4to induce an M2 phenotype. Leukocytes were then Amaxa-electroporated 2×10^6 HL-60 cells/100 μL in nucleofector and transfected with either 100 nM (final concentration) of either scrambled siRNA (control), or PLD1 siRNA (PC-PLD1 siRNA, catalog sc-4400), or PLD2 siRNA (PC-PLD1 siRNA, catalog sc-4401), from Santa Cruz Biotechnology, Inc., Dallas, TX. Control siRNA is a 19 bp scrambled sequence with 3′ dT overhangs certified not to have significant homology to any known gene sequences from mouse, rat or human and causes no significant changes in gene expression of transfected cells after 48 h at the same concentration as the siRNA in test. After nucleofection, cells were immediately plated into 6-well plates and incubated at 37°C for 48 h to allow for maximum gene expression silencing.

2.15 | Neutrophil superoxide release

Neutrophil ROS production, specifically, superoxide anion release was measured by the reduction of cytochrome *c* with several neutrophil agonists as indicated, with PMA (50 ng/mL) as the positive control and SOD was used to stop the reactions.

2.16 | Leukocyte chemotaxis

Chemotaxis against IL-8 (10 nM; neutrophils) or MCP-1 (30 nM; macrophages) was measured in Transwell (5 μm diameter pore for neutrophil, 8 μm diameter pore for macrophage) for specified lengths of time; cells migrated at the bottom of the wells were stained and counted. Averages from 7 fields were plotted.

2.17 | Macrophage phagocytosis

Macrophage phagocytosis was determined using fluorescent-labeled GFP zymosan A (*Saccharomyces cerevisiae*) (Invitrogen, Carlsbad, CA) as in Ref. 37. Briefly, the particles were opsonized at 37°C for 1h using the zymosan A BioParticles opsonizing reagent (derived from highly purified rabbit polyclonal IgG antibodies) (Invitrogen) and were applied to 1×10^7 cells such that there were approximately 20 zymosan particles per each cell. After application of GFP-Zymosan, the 6-well plates containing the cells were centrifuged at 800×g for 5 min and then were incubated at 37°C for 15 min. Fluorescent-labeled zymosan particles ingested by macrophages were counted manually under the microscope in 5 different fields, and the averages and SEM calculated.

2.18 | Neutrophil-extracellular traps

To detect NETs in the airway, cell-free supernatant of BAL fluid was used to quantify extracellular DNA citrullinated histone H3, which is a well-established marker of NETs. QuantIt Picogreen DNA quantification assay was used for the quantification of DNA. Rabbit

anti-citrullinated histone H3 (citH3) (ab5103; Abcam, Cambridge, MA, USA) was used to perform immunoblots.

2.19 | Statistical analysis

All data are expressed as means ± SEM. Comparisons between groups were conducted using ANOVA and Student's *t*-test as appropriate. A level of $P \leq 0.05$ was considered to indicate statistical significance. Statistics were performed using Graphpad Prism 6.0 for Windows (San Diego, CA).

3 | RESULTS

3.1 | PLD genes are regulated in patients with ARDS

To determine gene expression profiles in ARDS, microarray analysis was performed on peripheral blood obtained from patients with ARDS ($N = 19$) and from clinically matched patients without ARDS (Non-ARDS, $N = 29$) enrolled in a RoCI (Table 1). In addition to PLD1 and PLD2, the expression profile of phospholipid phosphatases (PLPP), a family of genes that includes PA phosphatases, was determined (Supplemental Fig. S2a). Gene expression is represented in log2, where positive values represent increased expression, and negative values represent decreased expression. On presentation, gene expression of PLD1 was increased in patients with ARDS relative to Non-ARDS (log2 relative change = 0.91), and PLD2 expression was unchanged between the 2 groups (log2 relative change = −0.07; Fig. 1A). At day 7, PLD1 expression was similar between the 2 groups (PLD1 log2 relative change = 0.02), and PLD2 expression was slightly increased in ARDS patients (PLD2 log2 relative change = 0.23; Fig. 1B). Of note, the variance in PLD1 and PLD2 gene expression in ARDS patients on presentation showed little change from presentation to day 7; log2 relative change day 7/presentation was 0.07 for PLD1, and 0.13 for PLD2. To confirm these determinations in a replicate cohort, publicly available microarray datasets from patients with ARDS ($N = 99$) and controls ($N = 166$) were merged in silico and normalized (see Materials and Methods). Peripheral blood gene expression analysis showed increased PLD1 (8.4 log2 relative change) and PLD2 expression (6.0 log2 relative change) at presentation in patients with ARDS relative to controls (Fig. 1C). In addition, patients with ARDS demonstrated significantly higher PLD1 expression relative to PLD2 expression (1.11 log2 relative change). PLPP gene expression analysis in RoCI patients demonstrated selective regulation as well (Supplemental Figs. S2b and S2c). For example, PLPP2 expression in ARDS patients was increased on presentation (log2 relative change = 2.19; Supplemental Fig. S2b) and decreased on day 7 (log2 relative change = −0.48; Supplemental Fig. S2c).

3.2 | PLD1 and PLD2 are differentially expressed in human peripheral blood from ARDS survivors

To examine the relationship between gene expression and ARDS outcome, ARDS survivors were identified in the BWH RoCI, and peripheral blood gene expression at presentation was compared with ARDS nonsurvivors. PLD1 and PLD2 expression were changed 1.2 and −1.0 fold (log2) respectively in ARDS survivors (Fig. 1D). Of note, PLPP2 expression was also increased in ARDS survivors (1.84 log2 FC; Supplemental Fig. S2d). Together, these results indicate differential expression of PLD1 and PLD2 genes in peripheral blood leukocytes

from ARDS patients. Specifically, PLD1 expression was associated with survival, whereas PLD2 expression was associated with mortality in ARDS patients.

3.3 | *Pld1* and *Pld2* gene expression are differentially regulated in lungs after self-limited acute tissue injury

To further characterize the roles of these phospholipases in response to acute lung injury (ALI), lung *Pld1* and *Pld2* gene expression was determined after sterile lung injury using a model of ARDS from gastric acid aspiration, an important clinical risk factor for ARDS (see Materials and Methods; Fig. 2A). *Pld1* and *Pld2* were expressed in neutrophils, macrophages, epithelial cells, and endothelial cells, with relatively more *Pld2* expression in macrophages and endothelial cells (Supplemental Fig. S3). Lung *Pld1* expression significantly increased 2.91 fold (±0.72) relative to control (Fig. 2B), whereas lung *Pld2* expression significantly decreased 0.12 fold (±0.09; Fig. 2C). Expression of PLPP genes was also regulated; *Plpp1* and *Plpp2* expression increased 12.4 fold (±1.83; Fig. 2D) and 3.3 fold (±0.46; Fig. 2E) in injured lungs relative to control. *Plpp6* expression was also increased in injured lungs (Fig. 2F).

3.4 | PLD activity increases after ALI

We next examined total lung PLD activity and the relative contributions of *Pld* isoforms (see Materials and Methods). To this end, intra-bronchial acid was administered to wild-type mice (WT), *Pld1* deficient mice ($Pld1^{-/-}$), and *Pld2*-deficient mice ($Pld2^{-/-}$). At baseline, lungs from WT gave significantly higher PLD activity (1.39 ± 0.15) relative to lungs from $Pld1^{-/-}$ (0.36 ± 0.05) and $Pld2^{-/-}$ (0.62 ± 0.10; Fig. 3A). PLD activity was significantly increased 24 h after intrabronchial HCl in WT mice (2.34 ± 0.37; Fig. 3A). After injury, PLD activity in lungs from $Pld1^{-/-}$ (1.13 ± 0.18) and $Pld2^{-/-}$ (0.99 ± 0.16) also significantly increased but remained lower than lungs from WT (Fig. 3A).

3.5 | *Pld1* deficiency is associated with impaired barrier function after ALI

To determine the impact of *Pld* isoforms on alveolar barrier function after acid-induced lung injury, levels of extravasated albumin were quantified in the alveolar compartment. Albumin concentration in BAL fluid obtained 24 h after intrabronchial acid was significantly higher in $Pld1^{-/-}$ (10.9 μg/mg protein ± 1.3 SEM) relative to WT (5.5 μg/mg protein ± 1.4 SEM) and $Pld2^{-/-}$ (2.0 μg/mg protein ± 1.4 SEM; Fig. 3B). Because the WT control animals were not the result of heterozygote mating (see Materials and Methods), another line of evidence for PLD isoform specific actions was determined with selective inhibitors. A selective pharmacologic inhibitor of PLD1 increased extravasation of intravascular EBD into lung interstitium (Fig. 3C). Selective inhibition of PLD2 did not significantly impact barrier integrity after ALI (Fig. 3C). Histology obtained 24 h after acid administration showed demonstrable tissue leukocyte infiltration and alveolar and interstitial edema in the left lung of WT that were in sharp contrast to the uninjured right lung (Fig. 3D). Relative to WT mice, alveolar edema was worse in lungs from $Pld1^{-/-}$ mice, and diminished in lungs from $Pld2^{-/-}$ mice (Fig. 3C). Of interest, determination of BAL fluid cytokine levels 24 h after injury gave significantly higher levels of IL-1α and GM-CSF in $Pld2^{-/-}$ mice relative to $Pld1^{-/-}$ (Supplemental Fig. S4). IL-6 was increased in $Pld2^{-/-}$ mice relative to WT and

Pld1$^{-/-}$ mice but statistical significance was not reached. Levels of TNF α and IL-10 were not significantly different (Supplemental Fig. S4).

3.6 | *Pld2* deficiency is associated with increased leukocyte tissue infiltration after ALI

To determine the role of *Pld* isoforms in acute lung inflammation, cellular host responses were examined by flow cytometric analysis of total and differential leukocyte counts in BALF after intrabronchial HCl in *Pld1*$^{-/-}$, *Pld2*$^{-/-}$, and WT mice (Fig. 4A, as in Ref. 36). At baseline, total and differential leukocyte counts were similar between the 3 genotypes (Figs. 4B–4G). After injury, total leukocyte counts increased in *Pld2*$^{-/-}$ ($220.5 \pm 24.4 \times 10^3$ cells per BALF), whereas they decreased in WT ($97.2 \pm 12.7 \times 10^3$ cells per BALF) and were not significantly different in *Pld1*$^{-/-}$ ($132.4 \pm 17.3 \times 10^3$ cells per BALF; Fig. 4B). Neutrophil (Fig. 4C) and recruited macrophage (exMacs in Fig. 4F, and iMacs in Fig. 4G) counts increased, whereas resident alveolar macrophage counts decreased 24 h after injury (rAMs; Fig. 4E).

The difference in direction of total leukocyte responses to injury at this time point suggests *Pld* isoform-specific influence on neutrophil and macrophage responses (Fig. 4B). To this end, neutrophil and alveolar macrophage subset counts were compared after lung injury between genotypes. Total leukocyte counts were significantly higher in *Pld2*$^{-/-}$ relative to *Pld1*$^{-/-}$ ($P = 0.009$) and WT ($P = 0.0004$; Fig. 4B). Specifically, deficiency in *Pld2* was associated with increased BAL neutrophils relative to WT ($155 \pm 25.0 \times 10^3$ vs. $51.6 \pm 11.1 \times 10^3$ cells per BALF, $P = 0.003$; Fig. 4C) and *Pld1*$^{-/-}$ ($88.6 \pm 18.2 \times 10^3$ cells per BALF, $P = 0.04$; Fig. 4D), and increased total macrophage counts relative to WT ($94.9 \pm 12.0 \times 10^3$ vs. $59.0 \pm 8.2 \times 10^3$ cells per BALF, $P = 0.04$; Fig. 4D) and *Pld1*$^{-/-}$ ($61.3 \pm 6.8 \times 10^3$ cells per BALF, $P = 0.04$; Fig. 4D). Macrophage subset determination demonstrated that iMacs were significantly increased in BAL fluid from *Pld2*$^{-/-}$ relative to WT ($16.3 \pm 4.0 \times 10^3$ vs. $6.4 \pm 1.8 \times 10^3$ cells per BALF, $P = 0.05$; Fig. 4G), and trended higher relative to *Pld1*$^{-/-}$ ($7.4 \pm 1.4 \times 10^3$ cells per BALF, $P = 0.07$; Fig. 4D). ExMacs trended higher in *Pld2*$^{-/-}$ relative to WT ($13.7 \pm 2.3 \times 10^3$ vs. $7.1 \pm 1.5 \times 10^3$ cells per BALF, $P = 0.07$; Fig. 4F). Together, these results indicate that deficiency in *Pld2* is associated with increased neutrophil and iMac recruitment to injured lung.

3.7 | *Pld2* deficiency is associated with increased iMac-neutrophil interactions during experimental ARDS

Recruited alveolar macrophages, iMacs and ExMacs engage with neutrophils for efferocytosis.[36] To determine if *Pld2* regulates cell-cell interactions between macrophages and neutrophils, macrophage-bound neutrophils in BALF were quantified by flow cytometry (Fig. 5A, as in Ref. 36). Deficiency in *Pld2* was associated with significantly increased absolute Ly6G+ iMac counts relative to WT ($14.3 \pm 3.5 \times 10^3$ vs. $5.7 \pm 1.6 \times 10^3$ cells per BALF, $P = 0.04$; Fig. 5B), and higher percentage of iMacs that were Ly6G+ (87.4 ± 3.2 vs. $74.0 \pm 5.5\%$ of iMacs, $P = 0.05$; Fig. 5C). The absolute Ly6G+ exMacs counts appeared higher in *Pld2*$^{-/-}$ relative to WT ($16.3 \pm 3.9 \times 10^3$ vs. $8.4 \pm 1.7 \times 10^3$ cells per BALF, $P = 0.08$; Fig. 5D), and the percentage of exMAcs that were Ly6G+ was very high in both genotype groups (95.1 ± 1.3 vs. $91.6 \pm 2.6\%$ of exMacs, $P = 0.12$; Fig. 5E).

3.8 | PLD2 silencing enhances proresolving macrophage functions

Pld2 was associated with changes in murine macrophage recruitment and function in vivo (*vide supra*). To investigate the impact of PLD on macrophage responses to injury, phagocytosis and chemotaxis were determined in human M2 macrophages (see Materials and Methods). Decreased PLD1 gene expression was associated with decreased macrophage chemotaxis toward MCP-1 relative to control ($1.45 \pm 0\ 26 \times 10^3$ vs. $2.77 \pm 0.42 \times 10^3$ cells per HPF, $P = 0.01$), whereas decreased PLD2 gene expression again gave contrasting results with increased macrophage transmigration ($3.92 \pm 0.35 \times 10^3$ vs. $2.77 \pm 0.42 \times 10^3$ cells per HPF, $P = 0.03$) at 360 min after exposure to the chemoattractant (Fig. 6A). In addition, decreased PLD1 gene expression was associated with decreased phagocytosis of latex beads relative to control (2.94 ± 0.33 vs. 4.82 ± 0.37 particle per cell, $P = 0.043$), whereas decreased PLD2 gene expression gave the opposite response with increased phagocytosis (6.15 ± 0.64 vs. 4.82 ± 0.37 particle per cell, $P = 0.006$) (Fig. 6B).

3.9 | PLD2 silencing decreased ROS production

Pld2 deficiency was associated with increased neutrophil recruitment and decreased histologic injury after experimental ALI (Figs. 3 and 4). The impact of PLD on neutrophil chemotaxis and ROS production was determined (see Materials and Methods). Decreased PLD2 gene expression gave increased chemotaxis toward IL-8 relative to control ($55.8 \pm 4.5 \times 10^3$ vs. $44.0 \pm 2.3 \times 10^3$ cells per HPF, $P = 0.04$), at 180 min after addition of chemoattractant, whereas decreased PLD1 gene expression was associated with decreased chemotaxis relative to control ($28.4 \pm 2.6 \times 10^3$ vs. $44.2 \pm 3.1 \times 10^3$ cells per HPF, $P = 0.035$) at 120 min after addition of chemoattractant (Fig. 6C). Although DNA levels were increased in BAL fluid after intrabronchial acid (Supplemental Fig.S5a), NETs were not detected (Supplemental Fig. S5b). Neutrophil ROS production in response to the agonists FMLP and PMA was determined. F-MLP (50 ng/mL) and PMA (50 ng/mL) increased ROS production in control neutrophils (Fig. 6D). PLD1 gene expression did not significantly alter ROS production to agonists. In contrast, decreased PLD2 gene expression decreased ROS production to both agonists.

4 | DISCUSSION

Results presented herein indicate that PLD isoforms are differentially regulated after ARDS. PLD1 gene expression is upregulated in human peripheral blood from ARDS survivors, and in murine lungs after self-limited ALI. In addition, PLD1 deficiency was associated with increased alveolar barrier disruption and tissue injury, suggesting a protective role for PLD1 in ARDS. Moreover, PLD2 gene expression was associated with ARDS nonsurvivors and was down-regulated in murine lungs after self-limited ALI. *Pld2* deficiency was associated with decreased tissue injury, increased recruitment of proresolving macrophages with enhanced phagocytosis, and decreased ROS production by neutrophils. Together, these findings support a pathogenic role for PLD2 that operates in opposition to PLD1 in ARDS.

PLD1 and PLD2 are the enzymatically active members of the mammalian PLD superfamily that catalyze the hydrolysis of phosphatidylcholine, the most abundant membrane phospholipid, to generate choline and PA, a second messenger signaling lipid (PA).[10]

Although animal models and in vitro studies have revealed pathogenic roles for PLD1 and PLD2 in thrombotic disease, cancer, and inflammatory diseases such as sepsis,[38] potential roles in human ARDS had yet to be investigated.

Examination of a published human gene expression microarray dataset from our institution[15] has enabled here a targeted analysis of PLD and PLD-related gene expression in patients with ARDS. As the number of popular platforms to measure gene expression increases, the ability to compare and integrate gene expression measures across diverse platforms has become correspondingly important. Several studies have shown an overall concordance of gene expression measures across platforms.[39,40] A recent study led to development of a new approach to map probes across platforms, allowing investigators to map probes from different microarray platforms.[26] The application of this method to the BWH RoCI and publicly available ARDS microarray datasets has increased our power to detect regulation of PLD gene expression, and allowed for external confirmation of findings from the BWH RoCI.

Regulation of PLD gene expression in peripheral blood prompted the investigation of gene expression in diseased lung. As gene expression changes in ALI are comparable between animal models and human disease,[41] associations between gene expression and recovery from disease were determined in a self-limited mouse model of acid induced ALI an important cause of ARDS.[1] In this model, inflammation peaks and resolution processes are engaged 24 h after intrabronchial acid instillation. Lung PLD gene expression correlated with results from human peripheral blood microarray datasets, indicating that PLD responses to lung injury are systemic, and could serve as potential biomarkers. *Pld1* expression was increased during self-resolving lung injury, as was expression of *Plpp1* and *Plpp2*, correlating with the association between gene expression and survival in patients with ARDS. Similarly, decreased lung *Pld2* expression in ALI correlated with decreased PLD2 expression in peripheral blood from ARDS patients. Results of the survivor analyses suggested that loss of PLD1 was detrimental, whereas loss of PLD2 was protective.

Indeed, *Pld1* gene deletion was associated with worse tissue injury and barrier dysfunction relative to WT mice after intrabronchial acid-induced lung injury. Total PLD activity was decreased in both *Pld*-deficient animals, indicating that compensatory increases in activity from the other PLD isoform was an unlikely confounding factor. PLD1 was expressed by multiple cell types in the lung, and played important roles in processes central to the development of ALI, such as endothelial barrier function, clearance of alveolar edema, and neutrophil activation. PLD signaling results in ROS-mediated endothelial cytoskeletal dysfunction.[42] PLD1 activation by TGF-beta results in internalization of the epithelial sodium channel ENaC, which prevents clearance of alveolar edema and potentiates lung injury.[43] In addition, PLD1 activation is linked to superoxide anion generation,[5] and neutrophil adhesion.[6] Therefore, the detrimental effect of *Pld1* deletion is likely related to a separate process. Endothelial cells from *Pld1*$^{-/-}$ mice demonstrate decreased integrin-dependent cell adhesion, and migration on extracellular matrices with subsequent impairments in angiogenesis.[29] In addition, PLD1 regulates beta-catenin signaling,[9] a signaling pathway important for lung epithelial repair.[44] Intrabronchial acid targets the lung epithelium,[45] and loss of PLD1 could disrupt epithelial repair and augment barrier

dysfunction. In addition, the lack of impact of *Pld1*$^{-/-}$ on in vivo cytokine release suggests a direct action on cellular responses rather than an indirect action downstream of cytokines.

As suggested by PLD2 gene expression profiles in ARDS patients and in murine self-limited ALI, *Pld2* gene deletion was protective, and associated with less tissue injury. The *Pld2*$^{-/-}$ mice had significantly increased neutrophil recruitment relative to WT, and PLD2 gene knockdown of human neutrophils increased chemotaxis to IL-8. Increased tissue infiltration by PLD2-deficient neutrophils was also observed in models of pancreatitis,[11] colitis,[46] and ALI secondary to sepsis.[12] PLD2 deficiency is associated with increased NETosis and survival from sepsis-induced ALI.[12] DNA levels were increased here with self-limited ALI; however, NETosis was not identified and DNA levels did not differ significantly by *Pld* genotype.

Deficiency in *Pld2* increased macrophage recruitment as well. Further characterization of the alveolar macrophage population demonstrated increased recruitment of iMacs and exMacs. Interactions between these macrophage subtypes and neutrophils, indicators of ongoing efferocytosis,[36] were also increased in *Pld2*-deficient mice. These macrophage subtypes participate in efferocytosis of apoptotic neutrophils for resolution of ALI,[36] and release protective cytokines such as IL-1ra,[47] and IL-10.[48] In addition, PLD2 gene knockdown was associated with increased human macrophage transmigration and phagocytosis by cells of proresolving M2 phenotype.[3] These changes in macrophage functions related to PLD2 expression were associated with increased levels of IL-1α and GM-CSF, suggesting PLD2 signaling was upstream of macrophage cytokine expression. Indeed, GM-CSF regulates efferocytosis by alveolar macrophages after lung injury,[49,50] and IL-1α promotes CD11b^{Low} alveolar macrophage proliferation and differentiation into CD11b^{High} macrophages.[51] Together, these findings suggest a regulated interplay between PLD2 and select cytokines that influence macrophage functional responses.

In health, specialized proresolving lipid mediators restrain inflammatory responses and promote resolution of inflammation.[52] These enzymatically derived endogenous lipid mediators counter-regulate proinflammatory signals to prevent excessive cellular responses and bystander tissue injury. Of interest, lipoxin A_4 (LXA_4) inhibits PLD activity and NADPH oxidase assembly by targeting PLPP6.[8,53] Of note, activation of PLPP6 can decrease levels of presqualene diphosphate, an inhibitor of PLD, to facilitate neutrophil responses in inflammation[8] and ALI.[54] Results presented here demonstrated regulation of PLPP6 gene expression in both human and experimental ARDS, supporting a role for this signaling pathway in the control of lung inflammation. Investigation into potential roles for PLD isoform-specific interactions with PLPP6 in ALI remains to be defined.

In summary, our findings have uncovered pathogenic and protective signaling circuits centered on PLD that are isoform specific. Data from ARDS patients and a mammalian model of self-resolving ALI demonstrated that PLD1 expression was associated with protection from tissue injury and increased survival from ARDS, whereas PLD2 expression adversely impacted recruitment of proresolving macrophages and recovery from ALI. Characterization of these distinct pathways offers a potential new host-directed therapeutic approach to ARDS that emphasizes PLD signaling and actions that are isoform specific. The

opposing actions of PLD1 and PLD2 provide a mechanism for host tissues to regulate the intensity of inflammation and its resolution.

Supplementary Material

Refer to Web version on PubMed Central for supplementary material.

ACKNOWLEDGMENTS

We thank Troy Carlo, Ho Pan Sham, and Guangli Zhu for technical advice and assistance. This research was supported in part by the US National Institutes of Health K08-HL130540 (R.E.A.), R01-HL056653-14 (J.G.C.), and P01-GM095467 (B.D.L.). The content is solely the responsibility of the authors and does not necessarily reflect the official views of NHLBI, NIGMS, or the National Institutes of Health.

Abbreviations:

ALI	acute lung injury
ARDS	acute respiratory distress syndrome
BAL	bronchoalveolar lavage
EBD	Evans blue dye
HCl	hydrochloric acid
ICU	intensive care unit
NETs	neutrophil-extracellular traps
PA	phosphatidic acid
PLPP	phospholipid phosphatases
PLD	phospholipase D
ROS	reactive oxygen species
RoCI	Registry of Critical Illness
qRT-PCR	quantitative real-time PCR
WT	wild-type

REFERENCES

1. Bellani G, Laffey JG, Pham T, et al. Epidemiology, patterns of care, and mortality for patients with acute respiratory distress syndrome in intensive care units in 50 countries. JAMA. 2016;315(8):788–800. [PubMed: 26903337]
2. Kolaczkowska E, Kubes P. Neutrophil recruitment and function in health and inflammation. Nat Rev Immunol 2013;13(3):159–175. [PubMed: 23435331]
3. Aggarwal NR, King LS, D'Alessio FR. Diverse macrophage populations mediate acute lung inflammation and resolution. Am J Physiol Lung Cell Mol Physiol 2014;306(8):L709–25. [PubMed: 24508730]

4. Matthay MA,Ware LB, Zimmerman GA. The acute respiratory distress syndrome. J Clin Invest 2012;122(8):2731–2740. [PubMed: 22850883]
5. Levy BD, Hickey L, Morris AJ, et al. Novel polyisoprenyl phosphates block phospholipase D and human neutrophil activation in vitro and murine peritoneal inflammation in vivo. Br J Pharmacol 2005;146(3):344–351. [PubMed: 16041402]
6. Speranza F, Mahankali M, Henkels KM, Gomez-Cambronero J. The molecular basis of leukocyte adhesion involving phosphatidic acid and phospholipase D. J Biol Chem 2014;289(42):28885–28897. [PubMed: 25187519]
7. Gomez-Cambronero J, Kantonen S. A river runs through it: how autophagy, senescence, and phagocytosis could be linked to phospholipase D by Wnt signaling. J Leuk Biol 2014;96(5):779–784.
8. Levy BD, Fokin VV, Clark JM, Wakelam MJ, Petasis NA, Serhan CN. Polyisoprenyl phosphate (PIPP) signaling regulates phospholipase D activity: a 'stop' signaling switch for aspirin-triggered lipoxin A4. FASEB J 1999;13(8):903–911. [PubMed: 10224233]
9. Gomez-Cambronero J Phospholipase D in cell signaling: from a myriad of cell functions to cancer growth and metastasis. J Biol Chem 2014;289(33):22557–22566. [PubMed: 24990944]
10. Gomez-Cambronero J, Di Fulvio M, Knapek K. Understanding phospholipase D (PLD) using leukocytes: pLD involvement in cell adhesion and chemotaxis. J Leuk Biol 2007;82(2):272–281.
11. Ali WH, Chen Q, Delgiorno KE, et al. Deficiencies of the lipid-signaling enzymes phospholipase D1 and D2 alter cytoskeletal organization, macrophage phagocytosis, and cytokine-stimulated neutrophil recruitment. PloS One. 2013;8(1):e55325. [PubMed: 23383154]
12. Lee SK, Kim SD, Kook M, et al. Phospholipase D2 drives mortality in sepsis by inhibiting neutrophil extracellular trap formation and down-regulating CXCR2. J Exp Med 2015;212(9):1381–1390. [PubMed: 26282875]
13. Jenkins GM, Frohman MA. PhospholipaseD: a lipid centric review. Cell Mol Life Sci 2005;62(19-20):2305–2316. [PubMed: 16143829]
14. Nanjundan M,Possmayer F. Pulmonary phosphatidic acid phosphatase and lipid phosphate phosphohydrolase. Am J Physiol Lung Cell Mol Physiol 2003;284(1):L1–23. [PubMed: 12471011]
15. Dolinay T, Kim YS, Howrylak J, et al. Inflammasome-regulated cytokines are critical mediators of acute lung injury. Am J Respir Crit Care Med 2012;185(11):1225–1234. [PubMed: 22461369]
16. Levy MM, Fink MP, Marshall JC, et al. SCCM/ESICM/ACCP/ATS/SIS International Sepsis Definitions Conference. Crit Care Med 2001;31(4):1250–1256.
17. Bernard GR, Artigas A, Brigham KL, et al. The American-European Consensus Conference on ARDS. Definitions, mechanisms, relevant outcomes, and clinical trial coordination. Am J Respir Crit Care Med 1994;149(3 Pt 1):818–824. [PubMed: 7509706]
18. Ventilation with lower tidal volumes as compared with traditional tidal volumes for acute lung injury and the acute respiratory distress syndrome. The acute respiratory distress syndrome network. N Engl J Med 2000;342(18):1301–1308. [PubMed: 10793162]
19. Kollef KE, Reichley RM,Micek ST, Kollef MH. Themodified APACHE II score outperforms Curb65 pneumonia severity score as a predictor of 30-day mortality in patients with methicillin-resistant Staphylococcus aureus pneumonia. Chest. 2008;133(2):363–369. [PubMed: 17951615]
20. Howrylak JA, Dolinay T, Lucht L, et al. Discovery of the gene signature for acute lung injury in patients with sepsis. Physiol Genom 2009;37(2):133–139.
21. Wong HR, Shanley TP, Sakthivel B, et al. Genome-level expression profiles in pediatric septic shock indicate a role for altered zinc homeostasis in poor outcome. Physiol Genom 2007;30(2):146–155.
22. Ritchie ME, Phipson B, Wu D, et al. limma powers differential expression analyses for RNA-sequencing and microarray studies. Nucleic Acids Res 2015;43(7):e47. [PubMed: 25605792]
23. Gentleman RC, Carey VJ, Bates DM, et al. Bioconductor: open software development for computational biology and bioinformatics. Genome Biol 2004;5(10):R80. [PubMed: 15461798]
24. Durinck S, Moreau Y, Kasprzyk A, et al. BioMart and Bioconductor: a powerful link between biological databases and microarray data analysis. Bioinformatics. 2005;21(16):3439–3440. [PubMed: 16082012]

25. Durinck S, Spellman PT, Birney E, Huber W. Mapping identifiers for the integration of genomic datasets with the R/Bioconductor package biomaRt. Nat Protoc 2009;4(8):1184–1191. [PubMed: 19617889]
26. Lin SH, Beane L, Chasse D, Zhu KW, Mathey-Prevot B, Chang JT. Cross-platform prediction of gene expression signatures. PloS One. 2013;8(11):e79228. [PubMed: 24244455]
27. Rudy J, Valafar F. Empirical comparison of cross-platform normalization methods for gene expression data. BMC Bioinformatics. 2011;12:467. [PubMed: 22151536]
28. Oliveira TG, Chan RB, Tian H, et al. Phospholipase d2 ablation ameliorates Alzheimer's disease-linked synaptic dysfunction and cognitive deficits. J Neurosci 2010;30(49):16419–16428. [PubMed: 21147981]
29. Chen Q, Hongu T, Sato T, et al. Key roles for the lipid signaling enzyme phospholipase d1 in the tumor microenvironment during tumor angiogenesis and metastasis. Sci Signal. 2012;5(249):ra79. [PubMed: 23131846]
30. Thielmann I, Stegner D, Kraft P, et al. Redundant functions of phospholipases D1 and D2 in platelet alpha-granule release. J Thromb Haemostasis. 2012;10(11):2361–2372. [PubMed: 22974101]
31. Abdulnour RE, Dalli J, Colby JK, et al. Maresin 1 biosynthesis during platelet-neutrophil interactions is organ-protective. Proc Natl Acad Sci USA. 2014;111(46):16526–16531. [PubMed: 25369934]
32. Mahankali M, Peng HJ, Henkels KM, Dinauer MC, Gomez-Cambronero J. Phospholipase D2 (PLD2) is a guanine nucleotide exchange factor (GEF) for the GTPase Rac2. Proc Natl Acad Sci USA. 2011;108(49):19617–19622. [PubMed: 22106281]
33. Henkels KM, Boivin GP, Dudley ES, Berberich SJ, Gomez-Cambronero J. Phospholipase D (PLD) drives cell invasion, tumor growth and metastasis in a human breast cancer xenograph model. Oncogene. 2013;32(49):5551–5562. [PubMed: 23752189]
34. Liscovitch M, Czarny M, Fiucci G, Tang X. Phospholipase D: molecular and cell biology of a novel gene family. Biochem J 2000;345(Pt 3):401–415. [PubMed: 10642495]
35. Henkels KM, Muppani NR, Gomez-Cambronero J. PLD-Specific small-molecule inhibitors decrease tumor-associated macrophages and neutrophils infiltration in breast tumors and lung and liver metastases. PloS One. 2016;11(11):e0166553. [PubMed: 27851813]
36. Abdulnour RE, Sham HP, Douda DN, et al. Aspirin-triggered resolvin D1 is produced during self-resolving gram-negative bacterial pneumonia and regulates host immune responses for the resolution of lung inflammation. Mucosal Immunol 2016;9(5):1278–1287. [PubMed: 26647716]
37. Kantonen S, Hatton N,Mahankali M, et al. A novel phospholipase D2-Grb2-WASp heterotrimer regulates leukocyte phagocytosis in a two-step mechanism. Mol Cell Biol 2011;31(22):4524–4537. [PubMed: 21930784]
38. Nelson RK, Frohman MA. Physiological and pathophysiological roles for phospholipase D. J Lipid Res 2015;56(12):2229–2237. [PubMed: 25926691]
39. Woo Y, Affourtit J, Daigle S, et al. A comparison of cDNA, oligonucleotide, and Affymetrix GeneChip gene expression microarray platforms. J Biomol Tech 2004;15(4):276–284. [PubMed: 15585824]
40. Barnes M, Freudenberg J, Thompson S, Aronow B, Pavlidis P. Experimental comparison and cross-validation of the Affymetrix and Illumina gene expression analysis platforms. Nucleic Acids Res 2005;33(18):5914–5923. [PubMed: 16237126]
41. Sweeney TE, Lofgren S, Khatri P, Rogers AJ. Gene expression analysis to assess the relevance of rodent models to human lung injury. Am J Respir Cell Mol Biol 2017;57(2):184–192. [PubMed: 28324666]
42. Usatyuk PV, Kotha SR, Parinandi NL, Natarajan V. Phospholipase D signaling mediates reactive oxygen species-induced lung endothelial barrier dysfunction. Pulm Circ 2013;3(1):108–115. [PubMed: 23662182]
43. Peters DM, Vadasz I, Wujak L, et al. TGF-beta directs trafficking of the epithelial sodium channel ENaC which has implications for ion and fluid transport in acute lung injury. Proc Natl Acad Sci USA. 2014;111(3):E374–83. [PubMed: 24324142]

44. Zemans RL, Briones N, Campbell M, et al. Neutrophil transmigration triggers repair of the lung epithelium via beta-catenin signaling. Proc Natl Acad Sci USA. 2011;108(38):15990–15995. [PubMed: 21880956]
45. Matute-Bello G, Frevert CW, Martin TR. Animal models of acute lung injury. Am J Physiol Lung Cell Mol Physiol 2008;295(3):L379–99. [PubMed: 18621912]
46. Zhou G, Yu L, Yang W, Wu W, Fang L, Liu Z. Blockade of PLD2 ameliorates intestinal mucosal inflammation of inflammatory bowel disease. Mediat Inflamm 2016;2016:2543070.
47. Herold S, Tabar TS, Janssen H, et al. Exudate macrophages attenuate lung injury by the release of IL-1 receptor antagonist in gram-negative pneumonia. Am J Respir Crit Care Med 2011;183(10): 1380–1390. [PubMed: 21278303]
48. Aggarwal NR, Tsushima K, Eto Y, et al. Immunological priming requires regulatory T cells and IL-10-producing macrophages to accelerate resolution from severe lung inflammation. J Immunol 2014;192(9): 4453–4464. [PubMed: 24688024]
49. Shyamsundar M, McAuley DF, Ingram RJ, et al. Keratinocyte growth factor promotes epithelial survival and resolution in a human model of lung injury. Am J Respir Crit Care Med 2014;189(12):1520–1529. [PubMed: 24716610]
50. Berclaz PY, Shibata Y, Whitsett JA, Trapnell BC. GM-CSF, via PU.1, regulates alveolar macrophage Fcgamma R-mediated phagocytosis and the IL-18/IFN-gamma -mediated molecular connection between innate and adaptive immunity in the lung. Blood. 2002;100(12):4193–4200. [PubMed: 12393686]
51. Huaux F, Lo Re S, Giordano G, Uwambayinema F, Devosse R, Yakoub Y, et al. IL-1alpha induces CD11b(low) alveolar macrophage proliferation and maturation during granuloma formation. J Pathol 2015;235(5):698–709. [PubMed: 25421226]
52. Basil MC, Levy BD. Specialized pro-resolving mediators: endogenous regulators of infection and inflammation. Nat Rev Immunol 2015.
53. Carlo T,Kalwa H, Levy BD. 15-Epi-lipoxin A4 inhibits human neutrophil superoxide anion generation by regulating polyisoprenyl diphosphate phosphatase 1. FASEB J 2013;27(7):2733–2741. [PubMed: 23568778]
54. Bonnans C, Fukunaga K, Keledjian R, Petasis NA, Levy BD. Regulation of phosphatidylinositol 3-kinase by polyisoprenyl phosphates in neutrophil-mediated tissue injury. J Exp Med 2006;203(4): 857–863. [PubMed: 16567384]

Summary statement:

PLD isoforms are differentially associated with survival in patients with ARDS, and regulate host responses to acute lung injury.

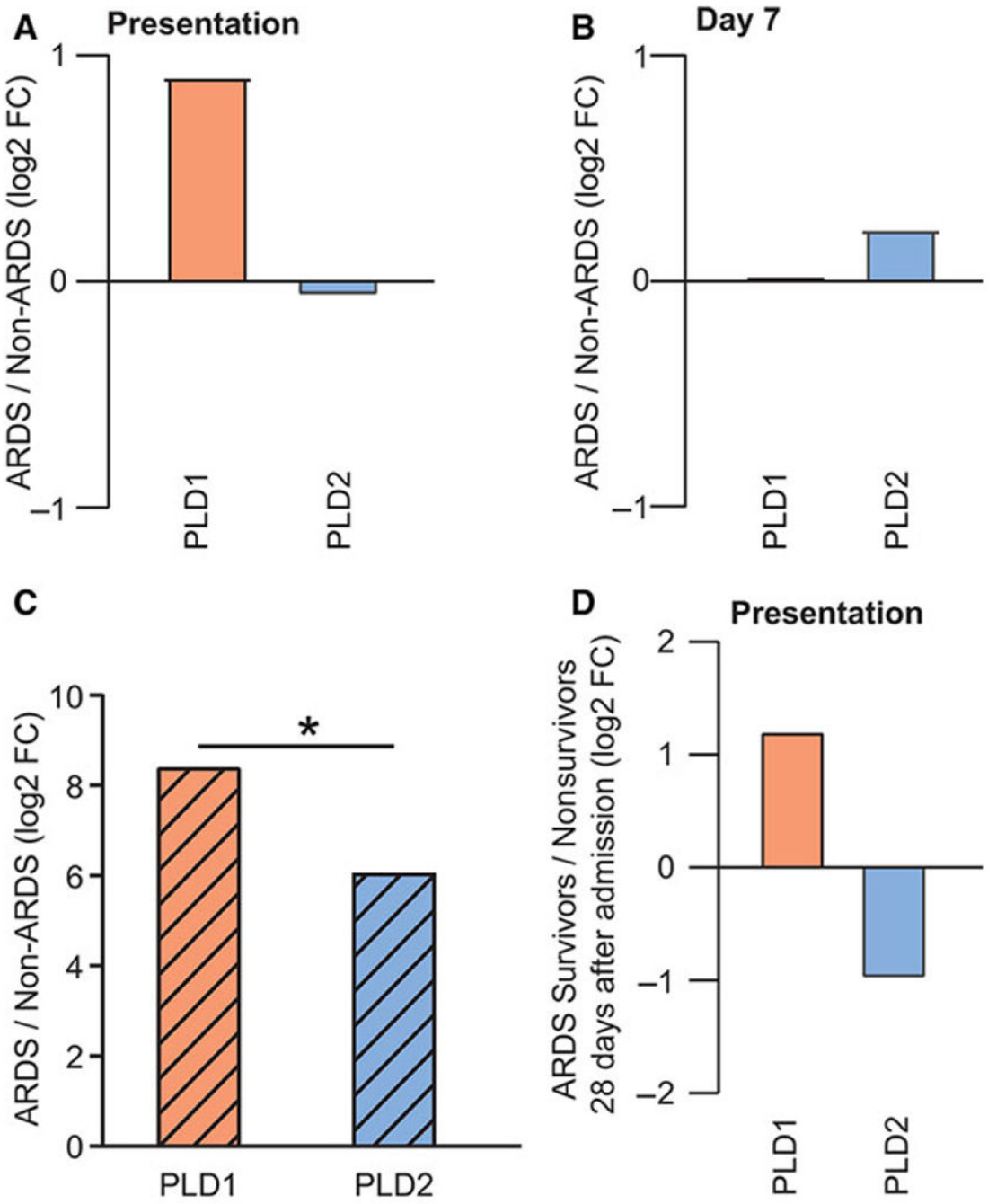

FIGURE 1. PLD genes are differentially regulated in peripheral blood during ARDS.

PLD1 and PLD2 gene expression fold change in ARDS/Non-ARDS (A) at presentation to the ICU, and (B) at day 7. (C) PLD1 and PLD2 gene expression fold change in ARDS/Non-ARDS patients from pooled microarray datasets obtained in external cohorts, $*P < 0.05$. (D) PLD1 and PLD2 gene expression fold change at presentation in ARDS survivors/ nonsurvivors. Gene expression is expressed in log2

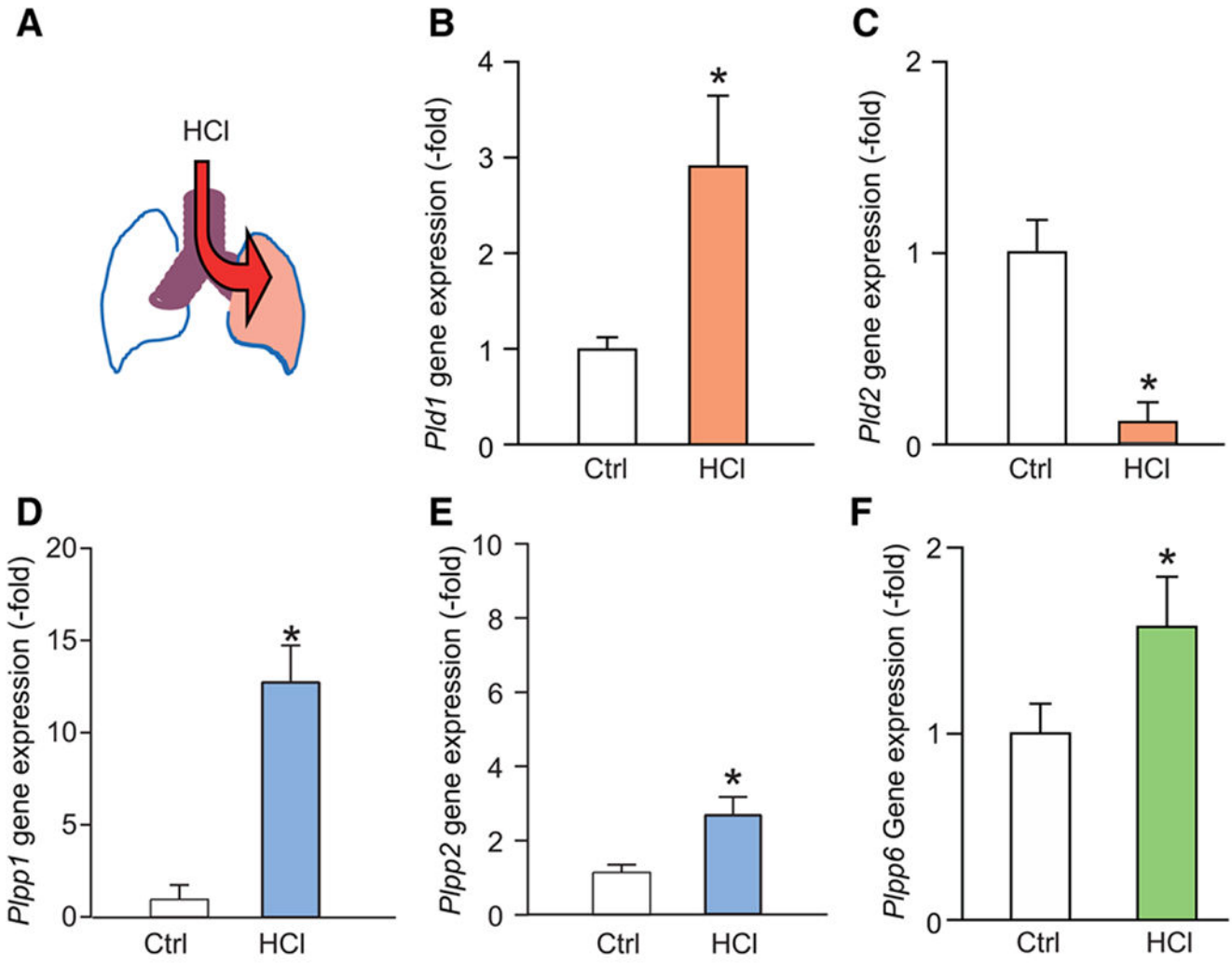

FIGURE 2. PLD isoforms and phospholipid phosphatase genes are differentially regulated in lungs after acute lung injury.

(A) Model of selective intratracheal HCl instillation to the left lung, and tissue harvesting at 24 h. Gene expression of (B) *Pld1*, (C) *Pld2*, (D) *Plpp1*, (E) *Plpp2*, and (F) *Plpp6* in control and lungs 24 h after intratracheal HCl. Gene expression is expressed in fold change relative to housekeeping gene (GAPDH, see Materials and Methods). Results are expressed as mean ± SEM, $N > 10$, $*P < 0.05$

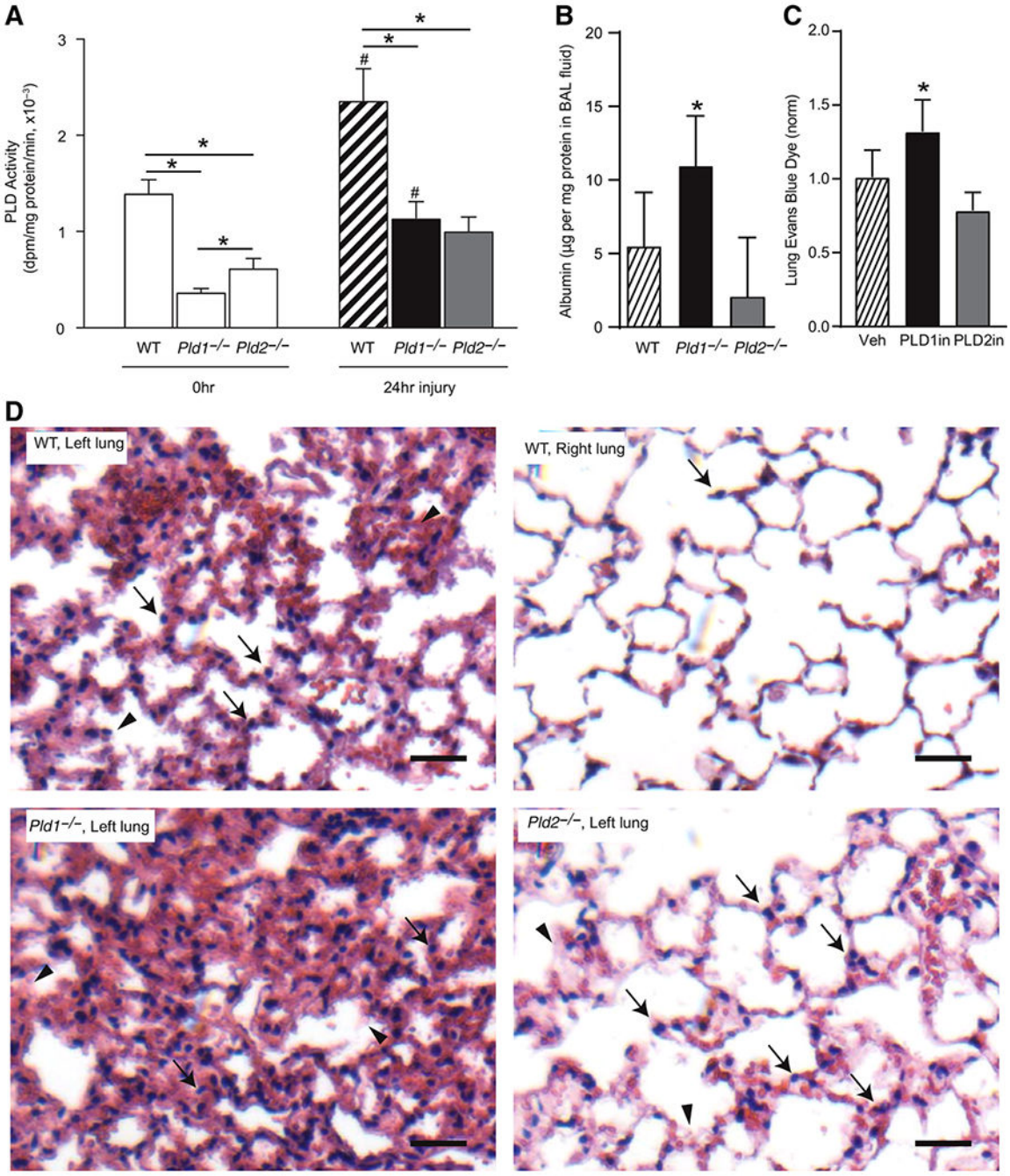

FIGURE 3. PLD deficiency impacts alveolar barrier disruption.

(A) Total lung PLD activity in wild-type (WT) mice, and mice deficient in *Pld1* and *Pld2* gene, at $t = 0$ and $t = 24$ h after intrabronchial HCl. Results are expressed as mean ± SEM, $N \geq 10$, $*P < 0.05$. (B) Albumin levels in BAL fluid from WT, $Pld1^{-/-}$, and $Pld2^{-/-}$ animals 24 h after intrabronchial HCl. (C) Evans blue dye levels in left lung homogenate 24 h after intrabronchial HCl and treatment with a selective inhibitor of PLD1 (PLD1in, black) or PLD2 (PLD2in, gray), or vehicle (Veh, hatched). Results are expressed as mean ± SEM, $N \geq$

10, *$P < 0.05$. (D) Representative lung sections from WT (injured left lung and uninjured right lung from same animal), *Pld1*$^{-/-}$, and *Pld2*$^{-/-}$ animals

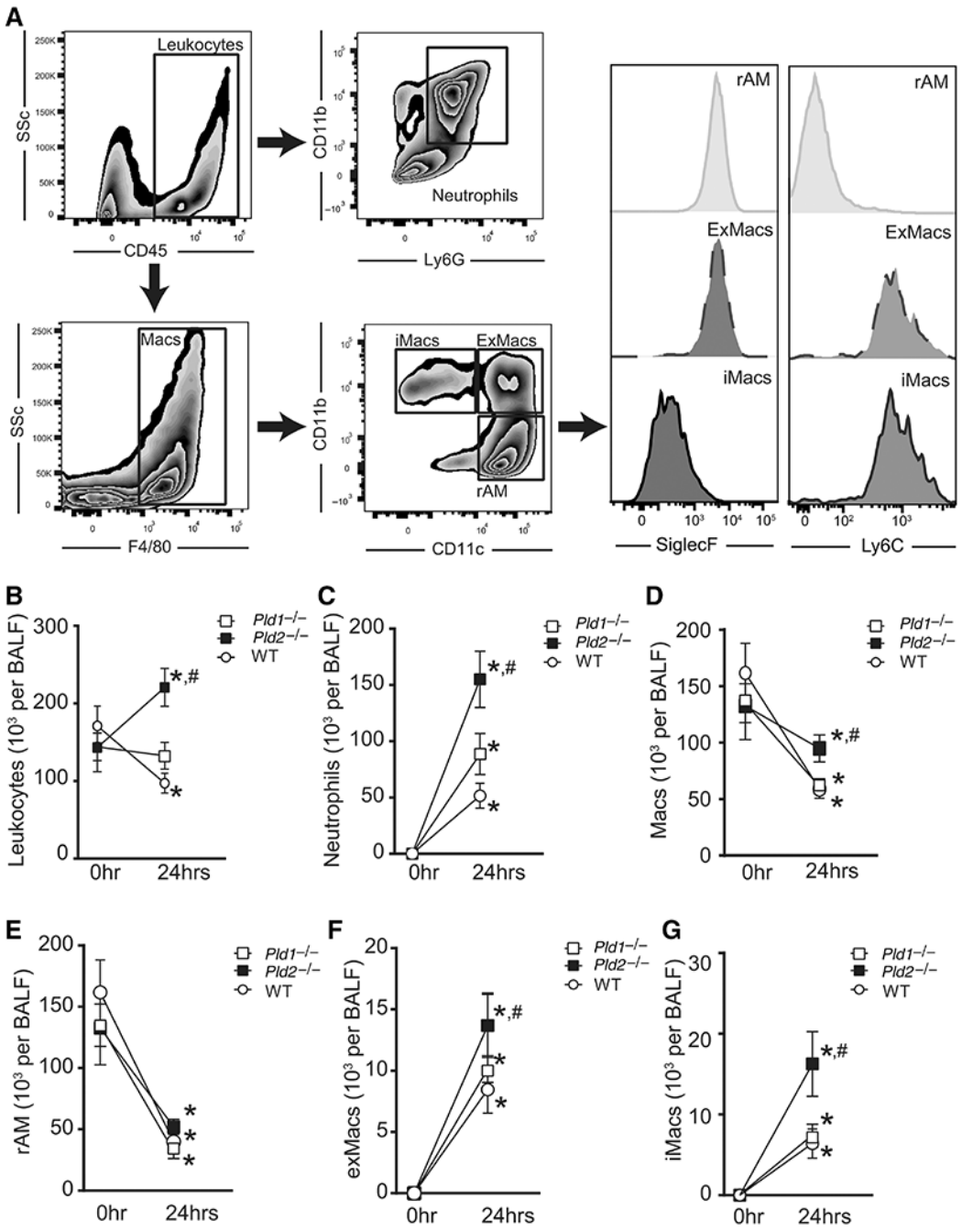

FIGURE 4. PLD1 and PLD2 regulate leukocyte recruitment after ALI.

(A) Representative flow cytometry dot plots and histograms from BAL gated on total cell population. Neutrophils, CD45+ CD11b+ Ly6G+; Macs, total macrophages, CD45+ F4/80+; iMacs; inflammatory macrophages, CD45+ F4/80+ CD11c− CD11b+ SiglecF− Ly6C+; exMacs; exudative macrophages, CD45+ F4/80+ CD11c+ CD11b+ SiglecF+ Ly6C+; rAM, resident alveolar macrophages, CD45+ F4/80+ CD11c+ CD11b− SiglecF+ Ly6C−. (B–G) Enumeration of (B) total cell count and differential cell count including (C) neutrophils, (D) total macrophages, (E) rAM, (F) ExMacs, and (G) iMacs, by flow cytometry analysis of

BAL fluid after intrabronchial acid. Results are expressed as mean ± SEM. n = > 10 per group. *P < 0.05

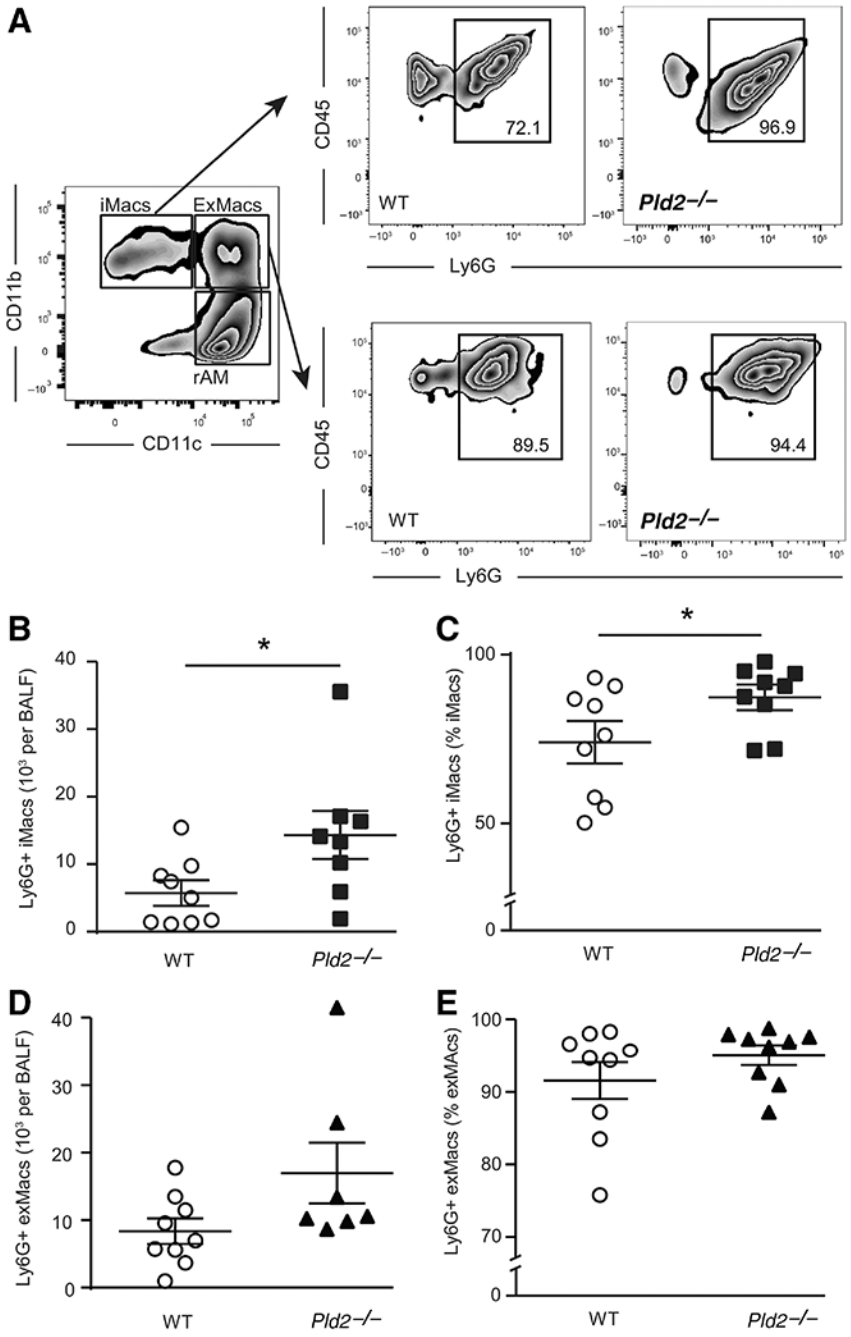

FIGURE 5. PLD genetic deficiency is associated with increased macrophage–neutrophil interactions.

(A) Representative dot plots of macrophage–neutrophil interactions as determined by Ly6G staining gated on macrophage subsets in BAL obtained 24 h after intrabronchial acid. (B) Absolute count and (C) percentage of iMacs that interact with neutrophils. (D) Absolute count and (E) percentage of exMacs that interact with neutrophils. Results are expressed as mean ± SEM. $n \geq 6$ per group. $^{*}P < 0.05$

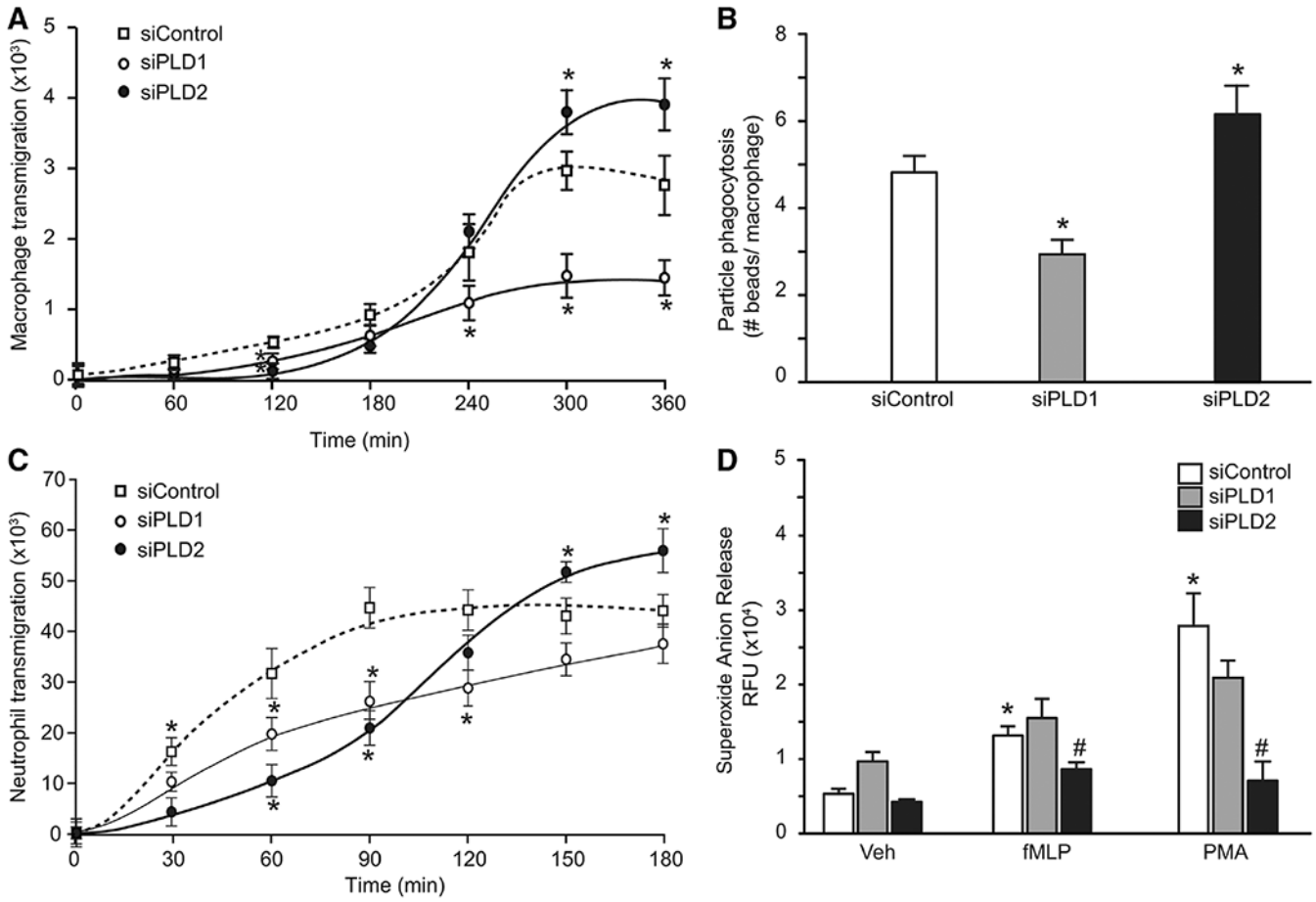

FIGURE 6. PLD isoform knockdown is associated with selective regulation of leukocyte function.

(A and B) Differentiated human M2 macrophages and neutrophils were transfected with either scrambled siRNA (controls), or a pool of PLD1 siRNAs, or a pool of PLD2 siRNAs (see Materials and Methods). (A) Chemotaxis across transwell membrane toward MCP-1(10 nM) was determined for the indicated lengths of time; cells migrated at the bottom of the wells were stained and counted. Averages from 7 fields were plotted. (B) Phagocytosis of green-fluorescent latex beads (0.1 mg/mL) was determined and expressed as the average of beads inside macrophages by fluorescence. (C and D) Differentiated human neutrophils were transfected with either scrambled siRNA (controls), or a pool of PLD1 siRNAs, or a pool of PLD2 siRNAs (see Materials and Methods). (C) Neutrophil transmigration across transwell membrane toward IL-8(10nM) was determined for the indicated lengths of time; cells migrated at the bottom of the wells were stained and counted. Averages from 7 fields were plotted. $*P < 0.05$ versus control. (D) Neutrophil superoxide anion release in response to vehicle (veh), f-MLP (150 nM), and PMA (50 ng/mL). Data presented are averages + SEM from 4 separate biologic experiments each in duplicate. $*P < 0.05$ versus veh, $\#P < 0.05$ versus siControl

TABLE 1

RoCI demographics

Diagnosis	**ARDS**	**Non-ARDS**	***P values***
Number of patients	19	29	
Age (yrs)	51	61	0.03
Sex (%M)	42.1	48.3	0.9
APACHEII (avg)	30	25	0.002
Hospital stay (days)	23	15	0.001
28-day mortality (%)	47.4	34.5	0.03